

TAU AND CHARM PHYSICS HIGHLIGHTS

P. ROUDEAU

Laboratoire de l'Accélérateur Linéaire,

CNRS-IN2P3 et Univ. de Paris-Sud, Bât. 200, BP 34 - 91898 Orsay cedex, France

E-mail: patrick.roudeau@cern.ch

In τ physics, we are at the frontier between the completion of the LEP program and the start of analyses from b -factories, which are expected to produce results in the coming years. Nice results from CLEO are steadily delivered in the meantime. For charm, impressive progress have been achieved by fixed target experiments in the search for CP violation and $D^0 - \bar{D}^0$ oscillations. First results from b -factories demonstrate the power of these facilities in such areas. The novel measurement of the D^* width by CLEO happens to be rather different from current expectations. The absence of a charm factory explains the lack or the very slow progress in the absolute scale determinations for charm decays.

1 Tau physics

τ physics is an extremely rich area. In the following, I will consider the tests of lepton couplings universality to weak vector bosons, in light of recent measurements. In a different domain, τ decays into two pions play a special role as they can be related to e^+e^- annihilation into hadrons (I=1 component) and thus provide an accurate determination of the pion form factor. It can be noted that, in τ decays, measurements are obtained within the same experimental running conditions and that hadronic decays are normalized relative to leptonic decays. These favourable circumstances allow, in general, a better control of systematics as compared with experiments operating at low energy e^+e^- machines which need to run at different energies and have to determine an absolute normalization for each energy point. These properties have been used to reduce uncertainties related to the virtual photon hadronic component in the evaluation of, for instance, the muon anomalous magnetic moment. Hadron production in τ decays, through the charged weak current, is theoretically "clean" and allows one to measure $\alpha_s(m_\tau^2)$ and to determine the value of the strange quark mass.

Because of the time allocated for this presentation, I was unable to cover other topics

such as the detailed spectroscopy of hadronic states in $n\pi$ ($n \geq 3$) decays, recent results on the Lorentz structure in leptonic decays¹ and new measurements of topological branching fractions².

Results presented in this review have been obtained by analysing a few 10^5 τ pairs in each LEP collaboration and a few 10^6 events in CLEO. In future a few 10^8 events will be available at b -factories.

1.1 Neutral current universality

LEP results have been finalized, the last analyses from ALEPH have been completed³. An important property of the τ lepton is that its polarisation can be measured from distributions of kinematical variables obtained from the four-momenta of its decay products. The variation of this polarization versus the angle (θ) between the τ^- and the incident electron beam directions (Eq. (1)) allows one to extract, separately, the electron (\mathcal{A}_e) and τ (\mathcal{A}_τ) asymmetries.

$$P_\tau(\cos\theta) = -\frac{\mathcal{A}_\tau(1 + \cos^2\theta) + \mathcal{A}_e(2\cos\theta)}{(1 + \cos^2\theta) + \frac{4}{3}\mathcal{A}_{FB}(2\cos\theta)} \quad (1)$$

with:

$$\mathcal{A}_l = \frac{2g_V^l g_A^l}{(g_V^l)^2 + (g_A^l)^2} \quad (2)$$

g_V^l and g_A^l are, respectively, the vector and axial vector couplings of the lepton (l) to the Z boson.

One may note, from figure 1, that all measurements are compatible and also that ALEPH results have the best accuracy. This comes mainly from a larger sample of analysed events (such as for instance $\tau^- \rightarrow a_1^- \nu_\tau$; $a_1^- \rightarrow \pi^- \pi^0 \pi^0$ decays) and from a better control of systematics. It is apparent also that the use of polarized beams from SLD, brings an important constraint on \mathcal{A}_e .

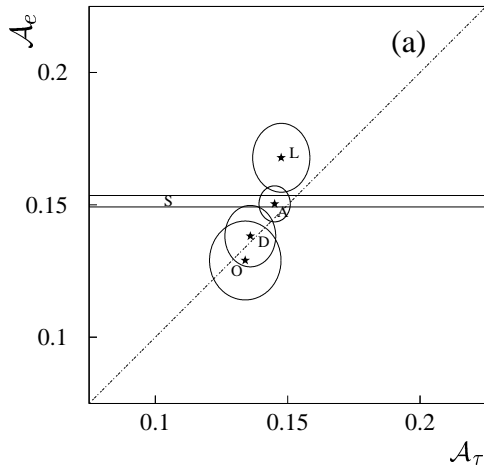


Figure 1. Comparison of the \mathcal{A}_e and \mathcal{A}_τ measurements by the ALEPH (A)³, DELPHI (D)⁴, L3 (L)⁵, and OPAL (O)⁶ collaborations. The ellipses are one standard error contours (39% CL). The horizontal lines represent the SLD (S)⁷ \mathcal{A}_e measurement plus and minus one standard deviation. Figure from ³.

The measurements of production rates, forward-backward asymmetries and, in case of τ leptons, of the polarization, can be used to extract values for the vector and axial-vector couplings of leptons to the Z boson. Figure 2 indicates that the three lepton families select compatible regions. In terms of accuracy, the τ has an intermediate position between the electron, which benefits from SLD ⁷ results on initial state polarization, and the muon for which no information on polarization is available. The overall average favours a rather light Higgs boson mass as is usually said.

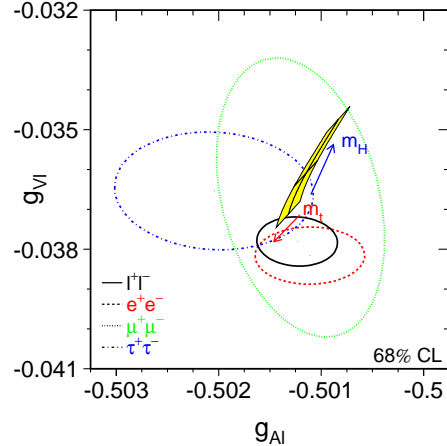


Figure 2. Effective lepton couplings. The ellipses are one standard deviation contours (39% CL). The shaded area indicates the Standard Model expectation. Figure from ⁸.

1.2 Charged current universality

Several measurements can be used to study the universality of lepton couplings to W bosons such as $\tau \rightarrow$ leptons, $\tau \rightarrow \pi(K)\nu_\tau$, ... in the following, among all possible tests, the most accurate results have only been considered.

τ leptonic decays have been measured into electron and muon final states. The present accuracies on the corresponding branching fractions are dominated by LEP results which are almost in their final form. The universality in charged current couplings can be studied, considering the parameters $g_{e,\mu,\tau}$ defined as:

$$G_{\tau\ell} = \frac{1}{\sqrt{2}} \left(\frac{g_\tau g_\ell}{4m_W^2} \right) = G_F \quad (3)$$

The theoretical expression for the leptonic τ branching fraction is then:

$$\text{BR}(\tau^- \rightarrow \ell^- \bar{\nu}_\ell \nu_\tau) = \frac{G_{\tau\ell}^2 m_\tau^5}{192\pi^3} f \left(\frac{m_\ell^2}{m_\tau^2} \right) \times \left(1 + \frac{3m_\tau^2}{5m_W^2} \right) (1 + \delta_{QED}) \quad (4)$$

In this expression, f , is a phase space correction to account for the final state charged lepton mass:

$$f(x) = 1 - 8x + 8x^3 - x^4 - 12x^2 \ln x \quad (5)$$

and δ_{QED} contains radiative corrections⁹:

$$\delta_{QED} = \frac{\alpha(m_\tau)}{2\pi} \left(\frac{25}{4} - \pi^2 \right) + 6.743 \left(\frac{\alpha(m_\tau)}{\pi} \right)^2. \quad (6)$$

From present averages¹⁰ of existing measurements:

$$\text{BR}(\tau^- \rightarrow e^- \bar{\nu}_e \nu_\tau) = (17.804 \pm 0.051)\% \quad (7)$$

$$\text{BR}(\tau^- \rightarrow \mu^- \bar{\nu}_\mu \nu_\tau) = (17.336 \pm 0.051)\% \quad (8)$$

and taking into account the expected difference coming from final lepton masses one obtains:

$$\frac{g_\mu}{g_e} = 1.0006 \pm 0.0021 \quad (9)$$

which can be compared with the value of 1.0023 ± 0.0016 deduced from measurements of $\pi \rightarrow \ell \bar{\nu}_\ell$ decays and using the determination of radiative corrections given in¹¹.

τ lifetime measurements at LEP are also almost final, the only remaining unpublished result, from DELPHI¹², has been delivered at this conference. The present accuracy on the τ lifetime is dominated by LEP experiments as illustrated in figure 3. It must be noted that the published CLEO result is from 1996, an updated analysis will have an improved accuracy. The equality of τ and μ couplings can be verified by comparing the value of the τ electronic branching fraction obtained within this hypothesis and the measured one:

$$\begin{aligned} \text{BR}_e^{th.} &= \left(\frac{m_\tau}{m_\mu} \right)^5 \frac{\tau_\tau}{\tau_\mu} \times 1.0005 \\ &= 0.17807 \pm 0.00061(\tau_\tau) \\ &\quad \pm 0.00015(m_\tau) \end{aligned} \quad (11)$$

$\text{BR}_e^{th.}$ has been obtained by applying Eq. (4) to $\tau^- \rightarrow e^- \bar{\nu}_e \nu_\tau$ and $\mu^- \rightarrow e^- \bar{\nu}_e \nu_\mu$, assuming $g_\tau = g_\mu$.

$$\text{BR}_e^{exp.} = 0.17814 \pm 0.00036 \quad (12)$$

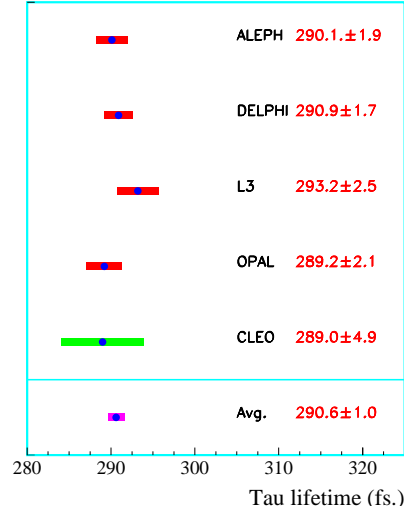


Figure 3. Present measurements of the τ lifetime and global average (units are fs).

These two values are in agreement and, because of the accurate determination of the τ lepton mass by BES¹³, the main uncertainty, in this comparison, is given by τ lifetime measurements. The experimental result, quoted in Eq. (12), is the average of the two values given in Eq. (7) and (8) and has been obtained assuming e - μ universality.

1.3 The $\tau^- \rightarrow \pi^- \pi^0 \nu_\tau$ channel

This decay mode of the τ lepton is of peculiar interest as it can be related to the two-pion channel produced in $e^+ - e^-$ annihilation, corresponding to isospin one final states, through the Conserved Vector Current hypothesis.

The C.V.C. hypothesis corresponds to the following equality between the spectral functions:

$$v_{I=1}^{\pi\pi}(q^2) = v^{\pi\pi^0}(q^2) \quad (CVC). \quad (13)$$

Spectral functions contain the decay dynamics and are defined in Eq. (10).

The electromagnetic pion form factor can be, in turn, related to these distributions

$$\frac{d\Gamma(\tau^- \rightarrow \pi^- \pi^0 \nu_\tau)}{dq^2} = \frac{G_F^2 |V_{ud}|^2 S_{EW}^{\pi\pi}}{32\pi^2 m_\tau^3} (m_\tau^2 - q^2)^2 (m_\tau^2 + 2q^2) v^{\pi\pi^0}(q^2)$$

$$\sigma(e^+e^- \rightarrow \pi^+\pi^-) = \left(\frac{4\pi^2\alpha_{em}^2}{s}\right) v^{\pi\pi}(s) \quad (10)$$

through the equality:

$$v^{\pi\pi}(q^2) = \frac{1}{12\pi} |F_\pi(q^2)|^2 \left(\frac{2p_\pi}{\sqrt{q^2}}\right)^3, \quad q^2 = m_{\pi\pi}^2 \quad (14)$$

It is normalized such that $F_\pi(0) = 1$. A recent model independent parametrization of the pion form factor, based on unitarity, analyticity and on the chiral behaviour of QCD at low energy, has been proposed¹⁴ which depends only on the ρ mass value. It is well in agreement with the measurements up to $q^2 \sim 1 \text{ GeV}^2$ as shown in figure 4. Such comparisons can be found also in the presentation of J. Bijnens at this Conference¹⁵.

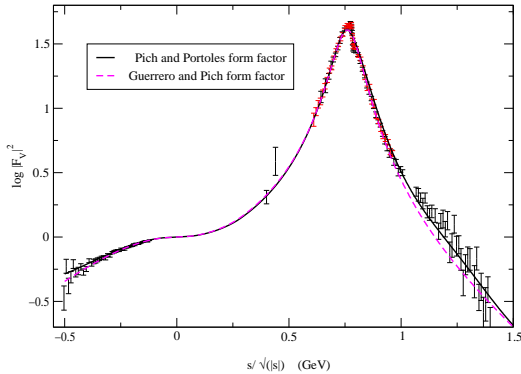


Figure 4. Comparison of the result of the fit explained in¹⁴ with the experimental data on $F_\pi(s)$ from $e^+e^- \rightarrow \pi^+\pi^-$ (time-like)¹⁶ and $e^-\pi^\pm \rightarrow e^-\pi^\pm$ (space-like)¹⁷. The result of the fit which has three parameters is compared with the parametrization¹⁸ which depends only on the value of the ρ mass. In the region below 0.8 GeV both curves are indistinguishable. Figure from¹⁴.

The most recent measurement, obtained by CLEO¹⁹, is shown in figure 5.

The C.V.C. hypothesis is expected to be violated at an extremely low level: $\mathcal{O}(m_u -$

$m_d)^2$. Experimentally, measurements obtained in τ decays and in $e^+ - e^-$ annihilation have to be corrected for I-spin violating effects coming from electromagnetic interactions as: $\omega^0 \rightarrow \pi^+\pi^-$, $m_{\pi^+} \neq m_{\pi^0}$ and $(m, \Gamma)_{\rho^-} \neq (m, \Gamma)_{\rho^0}$. After these corrections, the difference between the measured²⁰ $\tau^- \rightarrow \pi^- \pi^0 \nu_\tau$ branching fraction and the value deduced from $e^+ - e^-$ measurements, which includes new results from CMD-2²¹, is evaluated to be $(0.37 \pm 0.29)\%$ ²². It may be noted that the fitted mass value of the ρ meson $(775 \pm 1) \text{ MeV}/c^2$ is rather different from the present value quoted in the main section of PDG2000²³ which is $(769.3 \pm 0.8) \text{ MeV}/c^2$. This last value is dominated by results obtained in other experimental conditions than τ decays or $e^+ - e^-$ annihilation.

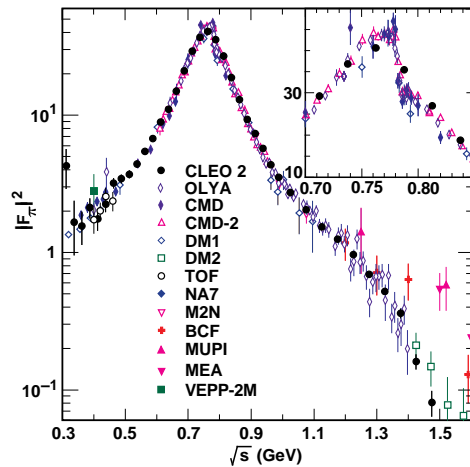


Figure 5. Comparison of $|F_\pi|^2$ as determined from CLEO data (filled circles), with that obtained from $e^+e^- \rightarrow \pi^+\pi^-$ cross sections (other symbols). The inset is a blow-up of the region near the ρ peak, where ρ - ω interference is evident in the e^+e^- data. Figure from¹⁹.

1.4 $\alpha_s(m_\tau^2)$ measurement

Studies of hadronic τ decays have been the basis of the most accurate measurement of the strong coupling constant.

First results on $\alpha_s(m_\tau^2)$ were obtained in 1993 from pioneer analyses done by ALEPH²⁴ which were based on theoretical developments²⁵ derived in the framework of the Operator Product Expansion formalism²⁶. The hadronic τ decay width, normalized to the leptonic width, R_τ , can be expressed, using the O.P.E. formalism in terms of a contour integral at $s \simeq m_\tau^2$.

$$R_\tau = 3 \left(|V_{ud}|^2 + |V_{us}|^2 \right) S_{EW} \times [1 + \delta'_{EW} + \delta^P + \delta^{NP}] \quad (15)$$

with: $S_{EW} = 1.0194$ and $\delta'_{EW} = 0.0010$. $S_{EW} = 1 + 2 \left(\frac{\alpha}{\pi} \right) \ln \frac{m_Z}{m_\tau}$ represents a short-distance correction due to virtual particles with energies ranging from m_τ to m_Z . Summing all leading logarithms of m_Z/m_τ gives the quoted value²⁷. The remaining radiative correction, $\delta'_{EW} = \frac{5}{12} \frac{\alpha(m_\tau)}{\pi}$, can be found in²⁸. From theory, it is expected that the dominant corrections to the naive expectation $R_\tau = N_c = 3$ originates from perturbative QCD:

$$\begin{aligned} \delta^P &= \frac{\alpha_s(m_\tau^2)}{\pi} + 5.2023 \left(\frac{\alpha_s(m_\tau^2)}{\pi} \right)^2 \\ &+ 26.366 \left(\frac{\alpha_s(m_\tau^2)}{\pi} \right)^3 \\ &+ (78.003 + K_4) \left(\frac{\alpha_s(m_\tau^2)}{\pi} \right)^4 \\ &+ \mathcal{O} \left(\frac{\alpha_s(m_\tau^2)}{\pi} \right)^5 \end{aligned} \quad (16)$$

K_4 is unknown, different estimates give a value of the order of 30, in the evaluation of systematic uncertainties, it has been assumed that K_4 varies within the range: 50 ± 50 . Corrections of non-perturbative origin are ex-

pected to be suppressed as m_τ^{-n} with $n \geq 2$:

$$\delta^{NP} \simeq \mathcal{O} \left(\frac{m_q}{m_\tau} \right)^2 + \sum_{D=4,6,\dots} C_D(\mu) \frac{\langle O \rangle_D}{m_\tau^D} \quad (17)$$

where $C_D(\mu)$ are short distance coefficients given by theory. The first term in this expression comes mainly from the value of the strange quark mass because effects from lighter quarks can be neglected. This property will be exploited in Sec. 1.5. Experimentally it is rather easy to measure R_τ as it depends only on the τ leptonic branching fraction:

$$\begin{aligned} R_\tau &= \frac{\Gamma(\tau \rightarrow X_h \nu_\tau)}{\Gamma(\tau^- \rightarrow e^- \bar{\nu}_e \nu_\tau)} = \frac{1}{B_e} - 1 - \frac{B_\mu}{B_e} \\ &= 3.641 \pm 0.011. \end{aligned} \quad (18)$$

Main progress during the past few years have consisted in measuring the dominant contributions from non-perturbative corrections²⁹⁻³⁰ demonstrating that they are under control. In this purpose, the three independent contributions to the hadronic final state, in τ decays, have been distinguished. The strange component, originating from Cabibbo suppressed $W^- \rightarrow \bar{u}s$ decays, has been isolated by considering events with an odd number of kaons. In this way, non-perturbative QCD corrections of order $\mathcal{O}(1/m_\tau^2)$ are eliminated, once corresponding events are removed from the analysis. The vector and axial-vector hadronic components are then separated by considering events with, respectively, an even or an odd number of pions. Corrections have to be applied to account for isospin violating decays of η and ω mesons and to distribute events with kaons³¹ over the two components. In a way, which is similar to the two pion final state, spectral functions can be defined which contain all the decay dynamics (see Eq. (19)).

Recent results, presented by OPAL³² are shown in figures 6 and 7. The dominant contributions of the ρ and a_1 mesons

$$v_1(s)/a_1(s) = \frac{m_\tau^2}{6 |V_{ud}|^2 S_{EW}} \frac{1}{\left(1 - \frac{s}{m_\tau^2}\right)^2 \left(1 + \frac{2s}{m_\tau^2}\right)} \frac{\text{BR}(\tau^- \rightarrow V^-/A^- \nu_\tau)}{\text{BR}(\tau^- \rightarrow e^- \bar{\nu}_e \nu_\tau)} \frac{1}{N_{V/A}} \frac{dN_{V/A}}{ds} \quad (19)$$

$$R_{V/A}^{kl} = \int_0^{s_0 \leq m_\tau^2} ds \left(1 - \frac{s}{m_\tau^2}\right)^k \left(\frac{s}{m_\tau^2}\right)^l \frac{dR_{V/A}}{ds} \quad (20)$$

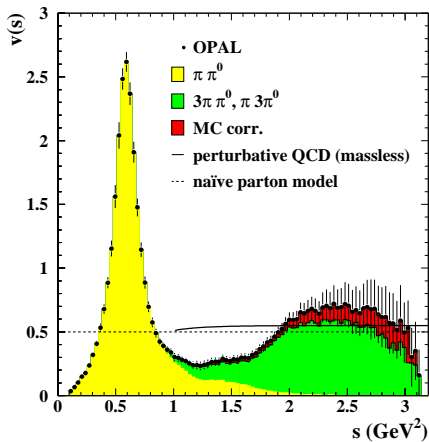


Figure 6. The vector spectral function measured by OPAL. Shown are the sums of all contributing channels as data points. Some exclusive contributions are shown as shaded areas. The naive parton model prediction is shown as dashed line, while the solid line depicts the perturbative, massless QCD prediction. Figure from ³².

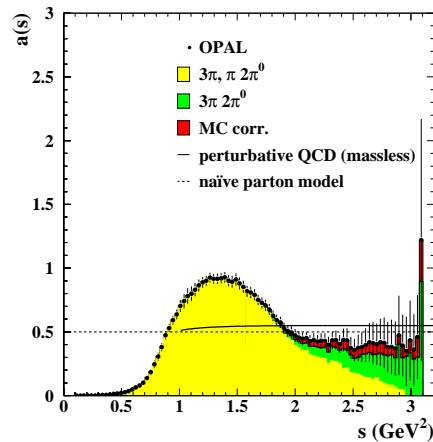


Figure 7. The axial-vector spectral function measured by OPAL. The same conventions have been used as in figure 6. The pion pole has been subtracted. Figure from ³².

are apparent, at low masses, respectively in the $v_1(s)$ and $a_1(s)$ spectral functions. It can be noted also that, at large mass values, the two functions are approaching the expectations from QCD. Differences relative to perturbative QCD evaluations are expected to be of non-perturbative origin and their contributions to R_τ have been parametrized in Eq. (17) using the O.P.E. formalism. Contributions from the different terms can be enhanced by considering moments of the spectral functions giving a larger weight to different regions of the mass distribution. In this way, coefficients C_D ($D = 4, 6, 8$) have been measured. The validity of this approach can

also be verified ³³ by considering “light- τ ” decays. Instead of evaluating the contour integral, which corresponds to expression (15), at $s = m_\tau^2$, the procedure is repeated for fixed values of s which are smaller than the τ mass and keeping only the parts of the spectral functions which satisfy this bound. Figure 8 illustrates the stability of the method down to hypothetic τ masses of the order of $1 \text{ GeV}/c^2$ when applied to the V+A spectral function. For individual V or A spectral functions the stability is observed over a lower range, down to $1.5 \text{ GeV}/c^2$.

The V+A combination appears to be peculiarly stable because of cancellations between the different non-perturbative contributions. From this analysis ³⁰, the following

CLEO ³⁵	ALEPH ³⁴	OPAL ³⁶
$(0.346 \pm 0.061)\%$	$(0.214 \pm 0.047)\%$	$(0.360 \pm 0.095)\%$

Table 1. Measured values for the $\tau^- \rightarrow K^- \pi^+ \pi^- \nu_\tau$ branching fraction.

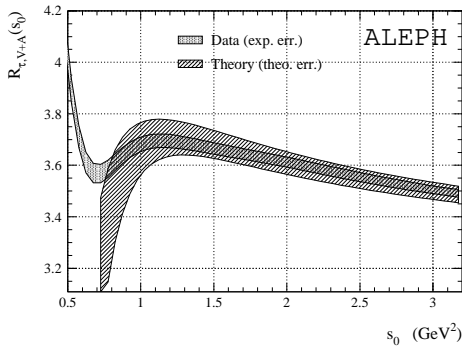


Figure 8. The ratio R_{V+A} versus the square of the “light- τ ” mass s_0 . The curves are plotted as error bands to emphasize their strong point-to-point correlations in s_0 . Also shown is the theoretical prediction. Figure from³⁰.

values have been obtained for the strong coupling constant, extrapolated from the τ up to the Z mass scales, and for the total contribution of non-perturbative effects:

$$\alpha_s(m_Z^2) = 0.1202 \pm 0.0008_{exp} \pm 0.0024_{th} \pm 0.0010_{extr} \quad (21)$$

$$\delta_{V+A}^{NP} = -0.003 \pm 0.005 \quad (22)$$

similar results have been obtained by CLEO²⁹ and OPAL³² collaborations.

1.5 Strange quark mass measurement

The analyses of τ spectral functions, described briefly in the previous section, can be sensitive to the value of the strange quark mass through non-perturbative corrections of order $(m_s/m_\tau)^2$. This sensitivity can be enhanced by isolating τ decays with an odd number of kaons. Several branching fractions of such channels have been measured mainly by ALEPH³⁴, CLEO³⁵ and OPAL³⁶ collaborations. One may note that there is not

a perfect agreement on the values obtained for the easiest channel ($\tau^- \rightarrow K^- \pi^+ \pi^- \nu_\tau$) by these three experiments (Table 1).

ALEPH³⁷ has also measured the spectral function in $\tau^- \rightarrow \bar{u}s\nu_\tau$ decays. To reduce the effects from perturbative QCD corrections, the following difference between moments is used:

$$\delta R^{kl} = \frac{R_{V+A}^{kl}}{|V_{ud}|^2} - \frac{R_S^{kl}}{|V_{us}|^2} \quad (23)$$

which is zero in the SU(3) limit. Figure 9 shows the hadronic mass dependence of δR^{00} .

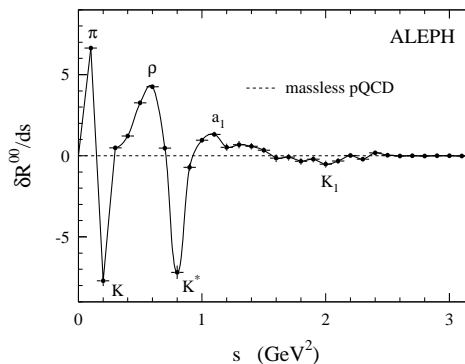


Figure 9. Value of Eq. (23) corresponding to the difference between Cabibbo-corrected nonstrange and strange invariant mass spectra. To guide the eye, the solid line interpolates between the bins of constant 0.1 GeV^2 width. Figure from³⁷.

The main difficulty, in this analysis, comes from the poor convergence of the perturbative QCD series which depends on the strange quark mass. This convergence depends on the choice of the values for k and l indices and a better convergence can be obtained at the expense of a lower experimental sensitivity to m_s . The origin of the convergence problem has been explained in³⁸. One can quote the two values from recent results^{39 40}, obtained for different choices of the k

$$a_\mu^{had} = \frac{\alpha^2(0)}{3\pi^3} \int_{4m_\pi^2}^{\infty} ds \frac{K(s)}{s} R(s); \quad R(s) = \frac{\sigma(e^+e^- \rightarrow had.)}{\sigma(e^+e^- \rightarrow \mu^+\mu^-)} \quad (24)$$

and l indices and which appear to be quite compatible:

$$m_s(m_\tau^2) = (120 \pm 11_{exp} \pm 8_{|V_{us}|} \pm 19_{th})$$

or

$$m_s(m_\tau^2) = (130 \pm 27_{exp} \pm 9_{th}) \quad (25)$$

(values are given in MeV/c² units).

This is an important result which improves the determination of the strange quark mass value and also of values for lighter quark masses once the ratio $m_s/(m_u+m_d)$ has been taken from analyses based on chiral perturbation theory⁴¹.

With larger statistics of Cabibbo suppressed τ decays, more accurate determinations of the strange quark mass can be obtained in future.

1.6 τ decays and $g-2$

The anomalous muon magnetic moment $a_\mu = \frac{g_\mu-2}{2}$ has been recently measured⁴² with improved accuracy and a further reduction of experimental uncertainties is still expected. To find evidence for new physics, this measurement has to be compared with theoretical expectations. The evaluation of a_μ receives three contributions, respectively, from pure quantum electrodynamics corrections, from the photon hadronic component and from W , Z or H exchange:

$$a_\mu = (a_\mu^{QED}(\pm 3) + a_\mu^{had}(\pm 150) + a_\mu^{weak}(\pm 4)) \times 10^{-11}. \quad (26)$$

The main uncertainty comes from the second component which, itself, can be splitted into two contributions: one being due to the photon hadronic vacuum polarization and the other which is usually named hadronic light-by-light scattering has to be determined from theory¹⁵. The former contribution is obtained by relating its value to the $e^+ - e^-$

hadronic annihilation cross section at low energy (see Eq. (24)).

The expression for $K(s)$ can be found for instance in⁴³ and it appears that 90% of the integral (24) corresponds to values of the energy below 1.8 GeV. The uncertainty quoted in Eq. (26) corresponds to the analysis⁴³ which is based on results from $e^+ - e^-$ annihilation at low energies, prior to 1995. Measurements of τ decays, explained in Sec. 1.3, can be used to complement results from $e^+ - e^-$ machines, at low energy. In addition, as $e^+ - e^-$ data, available at that time, were incomplete and suffer from systematics, properties of QCD such as unitarity and analyticity can be used in the framework of the O.P.E. to apply constraints. This approach⁴⁴ is rather similar to the one followed in Sec. 1.4. For a value of the energy higher than a typical hadronic scale, taken to be equal to 1.8 GeV, the ratio $R(s_0)$ can be expressed as a contour integral of analytical expressions obtained from perturbative QCD and from a parametrization on Non-Perturbative contributions in terms of series in s_0^{-n} :

$$R(s_0) = \frac{1}{2i\pi} \oint_{|s|=s_0} \frac{ds}{s} D(s). \quad (27)$$

$D(s)$ is the Adler D-function⁴⁵. Moments can be also defined, in a way similar as in Eq. (20) and mean values of the operators corresponding to the dominant non-perturbative components can be obtained. In this approach⁴⁴, the uncertainty on a_μ^{had} is reduced by a factor two with respect to Eq. (26), becoming equal to $\pm 75 \times 10^{-11}$.

This procedure is not applied in the region of resonances, below 1.8 GeV and in the vicinity of charm or beauty thresholds. Further constraints from QCD can be used in these regions, originating from QCD sum

$$\int_{4m_\pi^2}^{s_0} ds f(s) \Im \Pi = \underbrace{\int_{4m_\pi^2}^{s_0} ds [f(s) - P_n(s)] \Im \Pi}_{data} + \underbrace{\frac{i}{2} \oint_{|s|=s_0} ds P_n(s) \Pi^{QCD}}_{theory} \quad (28)$$

Energy (GeV)	$a_\mu^{had} \times 10^{11}$
$(2m_\pi - 1.8)_{uds}$	$6343 \pm 56_{exp} \pm 21_{theo}$
$(1.8 - 3.7)_{udsc}$	$338.7 \pm 4.6_{theo}$
$\psi(1S, 2S, 3770) + (3.7 - 5.0)_{udsc}$	$143.1 \pm 5.0_{exp} \pm 2.1_{theo}$
$(5.0 - 9.3)_{udsc}$	$68.7 \pm 1.1_{theo}$
$(9.3 - 12)_{udscb}$	$12.1 \pm 0.5_{theo}$
$(12 - \infty)_{udscb}$	$18 \pm 0.1_{theo}$
All	$6924 \pm 56 \pm 26$

Table 2. Contributions to a_μ^{had} from the different energy regions. The subscripts in the first column give the quark flavours involved in the calculation. Table taken from ⁴⁷.

rules. This method is explained in ⁴⁶. It consists in minimizing uncertainties from experimental results, at the expense of introducing theoretical uncertainties. Polynomial expressions are determined that mimic the singular weight function $K(s)/s$ in Eq. (24). This polynomial function is subtracted to decrease the importance of the dispersion integral which is evaluated from experimental measurements. In order to compensate for this subtraction (see Eq. (28)) the same polynomial function is added again, but now, being analytic, its contribution is evaluated on a circular contour in the complex plane, using a theoretical expression for the other part of the quantity to integrate.

Contributions to a_μ^{had} from different energy regions of the $e^+ - e^-$ hadronic annihilation cross section, obtained in the analysis of ⁴⁷, are given in Table 2. The total uncertainty on a_μ^{had} becomes equal to $\pm 62 \times 10^{-11}$ and is dominated by experimental uncertainties.

In a recent analysis ⁴⁸, which includes new and more accurate measurements from low energy $e^+ - e^-$ experiments (CMD-2 ²¹ and BES ⁴⁹) but in which constraints from QCD sum rules are not applied, very similar results have been obtained for the central

value and uncertainty of a_μ^{had} .

To improve further in the determination of a_μ^{had} , additional measurements at low energy, of $e^+ - e^-$ hadronic annihilation cross sections and τ decays, with a few 10^{-3} accuracy are needed.

2 Charm physics

Ideally, charm physics is an extraordinary place, for testing QCD technologies ⁵⁰ as lattice QCD, QCD sum rules or chiral theory because very accurate measurements can be obtained in charm decays on several key channels. It can be also considered to extrapolate such results to B physics in which the measurement of corresponding Cabibbo-Kobayashi-Maskawa matrix elements requires, usually, a good control of effects from strong interactions. For instance, at present, the most sensible way to evaluate the b -meson decay constant is through the measurement of the c -meson decay constant and lattice QCD ⁵¹. The present situation will be summarized in the following and it will be explained why such a program has not really started in practice. Another aspect of charm physics is the search for new phenomena. Direct searches on $D^0 - \bar{D}^0$ oscillations

Experiment	Operation	$\#D^0 \rightarrow K^- \pi^+$	σ_t/τ_{D^0}	$\sigma(\Delta m)$ (MeV)
E791	π^- 500 GeV	$\sim 4 \cdot 10^4$	few %	
FOCUS (E831)	$\gamma \leq 300$ GeV	$\sim 10^5$	$\leq 10\%$	~ 0.7
SELEX (E781)	π, Σ 600 GeV		4%	
CLEO	$e^+e^- \sqrt{s} = 10.6$ GeV	$\sim 2 - 4 \cdot 10^4$	$\sim 40\%$	~ 0.2
BaBar	$e^+e^- \sqrt{s} = 10.6$ GeV	$\sim 5 \cdot 10^4$	$\sim 40\%$	~ 0.3
BELLE	$e^+e^- \sqrt{s} = 10.6$ GeV	$\sim 9 \cdot 10^4$	$\sim 40\%$	~ 0.3

Table 3. A few characteristics of experiments contributing in charm physics.

and on CP violation in c -meson decays have made impressive progress during the past two years. Another aspect is related to the possibility of finding new physics effects in other fields, as b -hadron decays, because of the control of hadronic effects gained from c -hadron studies. Studies of c -hadron decays are also a good place for the spectroscopy of hadrons made of light quarks. As an example, clean signals from scalar mesons (σ, κ) have been observed in D^+ decays⁵² but, because of lack of time, I cannot develop these interesting aspects.

2.1 Contributing experiments

A few key parameters illustrating different characteristics of charm production measured at fixed target experiments and at experiments running at the $\Upsilon(4S)$ are given in Table 3.

At present, statistics of reconstructed charm events are rather similar. This will change during the coming years with the increase of registered data at b -factories. Fixed target experiments had the advantage of measuring accurately the c -hadron decay time. This property is also crucial, in their analyses, to isolate clean events samples. Because of the higher relative production rate of charmed particles, of a better mass resolution and powerful particle identification, experiments at the $\Upsilon(4S)$ can obtain charm samples with similar purity even if their decay time resolution is 10 times lower. The exper-

imental mass resolution is also an important parameter, as explained in Sec. 2.5. Only CLEO and, possibly in future b -factories, seem to be in a position to measure the D^{*+} width.

2.2 Charm hadron lifetimes

Lifetime measurements are needed to relate experiments, which measure branching fractions, and theory, which predicts partial widths.

Within the O.P.E. formalism, the total decay width of a charmed hadron can be expressed as a series in $1/m_c$ ⁵³, the first contributing correction, related to differences between mesons and baryons, is of order $\mathcal{O}(1/m_c^2)$.

$$\begin{aligned} \Gamma(H_c) &= \Gamma_{spect.} + \mathcal{O}(1/m_c^2) \\ &+ \Gamma_{PI,WA,WS}(H_c) \\ &+ \mathcal{O}(1/m_c^4) \end{aligned} \quad (29)$$

The first term in Eq. (29) corresponds to the c -quark decay (spectator contribution). Mechanisms in which the light c -hadron constituents are involved are of order $\mathcal{O}(1/m_c^3)$ but can have large contributions because they are phase-space enhanced (by $16\pi^2$). These contributions are indicated in figure 10. Effects from weak annihilation (W.A.), contributing in D^0 and D_s decays are expected to be rather small as they are helicity suppressed. Largest effects are expected from Pauli interference (P.I.) which can be destructive and also constructive, in case of

lifetime ratio	mechanism
$\tau(D^+)/\tau(D^0) = 2.54 \pm 0.02$	P.I.(-)
$\tau(D_s^+)/\tau(D^0) = 1.206 \pm 0.013$? interf W.A./Spect.
$\tau(\Lambda_c^+)/\tau(D^0) = 0.49 \pm 0.01$	W.S., P.I.(-)
$\tau(\Xi_c^+)/\tau(\Lambda_c^+) = 2.25 \pm 0.14$	W.S., P.I.(±)

Table 4. Present values for c -hadron lifetime ratios. Expected dominant contributions which can explain deviations from unity of these ratios are indicated.

baryons, and from weak scattering (W.S.) which, for baryons, is no more helicity suppressed. These considerations are explained in ⁵³.

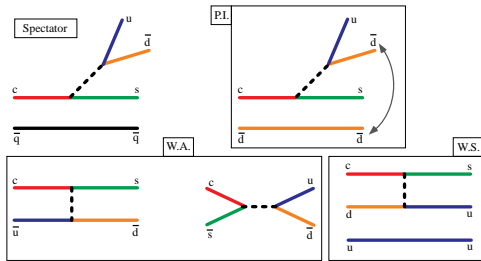


Figure 10. Idealized diagrams contributing in c -hadron decays. In the spectator graph, light partons are not contributing in the weak process. The Pauli interference (P.I.) graph is active when two identical partons are present in the final state. The weak annihilation (W.A.) graphs are helicity suppressed, whereas, for baryons the weak scattering (W.S.) is not.

At this conference new measurements (see figure 11) have been provided by BELLE ⁵⁴, CLEO ⁵⁵, FOCUS ⁵⁶ and SELEX ⁵⁷ collaborations. Some of these results have a statistical accuracy similar to or even better than the world average obtained in year 2000. Studies of systematic uncertainties are thus crucial and BELLE, for instance, has demonstrated that they can be controlled also at a very low level. An accuracy better than one % has been obtained on D^0 and D^+ lifetimes.

Taking the (naive) average of all measurements the obtained lifetime ratios are given in Table 4.

The D_s^+ lifetime is 20% larger than the D^0 lifetime. A difference of $\mathcal{O}(10\%)$ has been anticipated but neither its exact value nor its

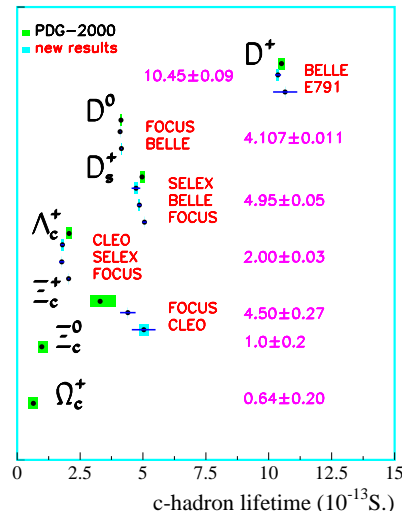


Figure 11. New measurements of c -hadron lifetimes are compared with PDG2000 averaged values (upper point given for each charmed hadron). For new results, points with error bars correspond respectively to the central values and statistical uncertainties. Shaded zones are for systematic uncertainties (they correspond to the total uncertainty in PDG averages).

sign were really predicted ⁵⁸. The other measured ratios can be used to evaluate the relative contributions from P.I. and W.S. mechanisms ^a.

$$\frac{\Gamma(P.I.)}{\Gamma(spec.)} \simeq 0.6$$

^aThis has been done very naively considering that the respective partial widths for these processes are independent of the type of the decaying c -hadron. It has been assumed also that P.I. has the same importance being constructive or destructive. Possible interferences between different mechanisms have not been either considered.

$$\frac{\Gamma(W.S.)}{\Gamma(spec.)} \simeq 1.6 \quad (30)$$

These values indicate that non-spectator effects are similar to the spectator contribution and not much larger. Thus, in spite of the rather low value of the c -quark mass, which is close to $1 \text{ GeV}/c^2$, the hierarchy of charm hadron lifetimes can be understood within the formalism illustrated by Eq. (29). To go further, absolute semileptonic branching fractions of c -hadrons, especially for the D_s^+ and c -baryons, need to be measured. The same formalism⁵⁹ predicts:

$$\Gamma_{sl}(\Omega_c^0) > \Gamma_{sl}(\Xi_c^+) \simeq \Gamma_{sl}(\Xi_c^0) \geq 2\Gamma_{sl}(\Lambda_c^+) \quad (32)$$

As an example, the Ξ_c^+ and Ξ_c^0 are expected to have similar semileptonic decay widths whereas their lifetimes differ by a factor five. It can be noted that new lifetime measurements^{60 61} have been obtained for the Ξ_c^+ which are significantly larger than the previous average.

2.3 CP violation

As it will clearly appear in Sec. 2.4, CP violation through mixing is expected to be very small for D^0 mesons. The search for effects from direct CP violation seems to be more promising. CP violation, in those circumstances, requires the contribution from two weak and two strong amplitudes in the decay process. The expression for the CP asymmetry is given in Eq. (31) in which A_i , δ_i^S and δ_i^W , $i = 1, 2$ are respectively the moduli, the strong and the weak phases of the two amplitudes.

Penguin graphs, in Cabibbo suppressed decays, are good candidates to provide the second weak amplitude. Other possibilities involve W.A. graphs in D_s^+ decays and channels with K_S^0 ⁶². Accurate predictions are difficult because they need to have a control on strong interaction phases. Typically, effects of $\mathcal{O}(10^{-3})$ are expected in several channels

⁶³. Present results of \mathcal{A}_{CP} are given in Table 5.

Impressive improvements^{64 65 66} have been obtained during the past two years. On some channels, the sensitivity is close to one % and systematic uncertainties do not seem to be the limiting factor. Another order of magnitude is needed to reach Standard Model expectations ... and more to expect a significant measurement. It can be noted that there are also interesting prospects to achieve high sensitivities in Cabibbo favoured channels (CLEO, FOCUS, b -factories) and in detailed studies of corresponding Dalitz plots (even time dependent) for conjugate states.

2.4 $D^0 - \bar{D}^0$ oscillations

Let's note that this is the only oscillating system involving a (relatively) heavy up-quark and consequently with d -type quarks circulating inside the loop (see figure 12). This

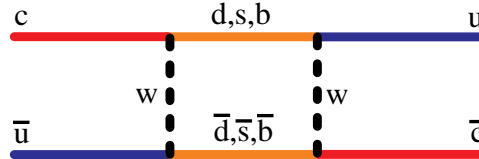


Figure 12. An example of a diagram contributing to $D^0 - \bar{D}^0$ oscillations.

type of diagram generates differences between the masses and the widths of the mass eigenstates of the $D^0 - \bar{D}^0$ system. For b - and s -hadrons, Δm dominates over $\Delta\Gamma$. For charm, contributions from d and s quarks, circulating inside the loop, are expected to be dominant as the values of the CKM matrix elements related to the b quark are extremely small. Standard Model expectations for the mass and width differences between the mass eigenstates of the $D^0 - \bar{D}^0$ system are extremely small⁶⁷:

$$\frac{\Delta\Gamma}{2\Gamma}|_{sd} \simeq \frac{\Delta m}{\Gamma}|_{sd} \simeq 10^{-4} - 10^{-5} \quad (33)$$

$$\mathcal{A}_{CP} = \frac{|A_f|^2 - |\bar{A}_f|^2}{|A_f|^2 + |\bar{A}_f|^2} = \frac{2\frac{A_2}{A_1} \sin(\delta_1^S - \delta_2^S) \sin(\delta_1^W - \delta_2^W)}{1 + \frac{A_2^2}{A_1^2} + 2\frac{A_2}{A_1} \cos(\delta_1^S - \delta_2^S) \cos(\delta_1^W - \delta_2^W)} \quad (31)$$

Channel	E791 ⁶⁴	CLEO ⁶⁵	FOCUS ⁶⁶	Average	Theory ⁶³
D ⁰ → K ⁻ K ⁺	-10 ± 50	0.5 ± 23	1 ± 27	6 ± 16	0.1 ± 0.8
D ⁰ → π ⁻ π ⁺	-49 ± 84	-19.5 ± 33.3	48 ± 46	22 ± 26	0.02 ± 0.01
D ⁰ → K _S ⁰ π ⁰		1 ± 13		1 ± 13	
D ⁰ → π ⁰ π ⁰		1 ± 48		1 ± 48	
D ⁺ → K ⁻ K ⁺ π ⁺	-14 ± 29		6 ± 12	2 ± 11	2 ± 1
D ⁺ → π ⁻ π ⁺ π ⁺	-17 ± 42			-17 ± 42	-1.2 ± 0.7
D ⁺ → K _S ⁰ π ⁺			-5 ± 14	-5 ± 14	
D ⁺ → K _S ⁰ K ⁺			42 ± 52	42 ± 52	

Table 5. Present measured values, in 10⁻³ units, of CP asymmetries.

Corrections from strong interactions can increase these values but not much apparently^{67 68}:

$$\frac{\Delta\Gamma}{2\Gamma}|_{ld,HQET} \simeq \frac{\Delta m}{\Gamma}|_{ld,HQET} \simeq 10^{-3} - 10^{-4} \quad (34)$$

New physics contributions are expected to enter more probably in Δm than in $\Delta\Gamma$ whereas non-perturbative QCD contributions, as for instance violations of parton-hadron duality, can contribute in the two quantities⁶⁸. From these considerations it results that:

- experimentally, measuring $\frac{\Delta m, \Delta\Gamma}{\Gamma} \leq 10^{-3}$ is quite challenging,
- theoretically, having done this measurement and found a signal or a limit at this level, is far from trivial, implying small effects from parton/hadron duality violation⁶⁸,
- it is necessary to measure Δm and $\Delta\Gamma$ in a separate way.

For a recent update on this subject see also⁶⁹.

Recent results have been obtained by BELLE⁷⁰ and CLEO⁶⁵ on $\Delta\Gamma$. These

analyses consist in measuring the lifetime for events corresponding to different combinations of mass eigenstates^b. For instance, K⁺K⁻ or π⁺π⁻ decay channels correspond to a CP (or mass) eigenstate whereas K⁻π⁺ contains the same fraction of the two mass eigenstates. The measured lifetimes (see figure 13) can be related to the decay width difference between the two mass eigenstates of the D⁰ - \bar{D}^0 system:

$$\frac{\Delta\Gamma}{2\Gamma} = \frac{\tau(K^-\pi^+)}{\tau(K^-K^+)} - 1 \quad (35)$$

The new measurements have not confirmed the positive effect seen by FOCUS⁷¹ as shown in figure 14. Averaging all results gives a value compatible with zero and it must be noted that the sensitivity has already reached 1% and does not seem to be limited by systematics. There are thus good prospects for improvements at *b*-factories.

Other types of measurements are sensitive both to Δm and $\Delta\Gamma$. They consist in comparing the time evolution of Cabibbo favoured (C.F.) and doubly Cabibbo suppressed (D.C.S.) decays. An example is given in Eq. (36) for the D⁰ → K⁻π⁺ channel.

^bIt has been assumed, in the following, that mass and CP eigenstates are the same.

$$R_{WS}(t) = \left| \frac{\langle K^- \pi^+ | \overline{D^0}(t) \rangle}{\langle K^- \pi^+ | D^0(t) \rangle} \right|^2 = R_{DCS} + \sqrt{R_{DCS}} y' \left(\frac{t}{\tau(D^0)} \right) + \frac{x'^2 + y'^2}{4} \left(\frac{t}{\tau(D^0)} \right)^2 \quad (36)$$

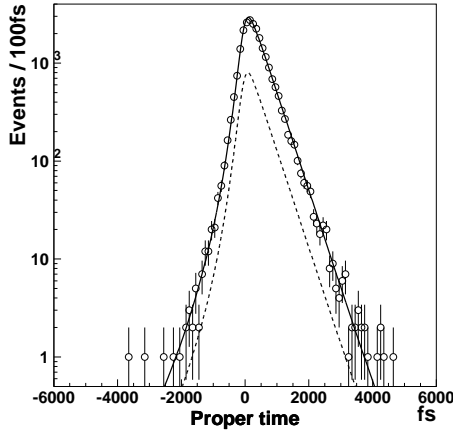


Figure 13. Proper-time distribution and lifetime fit result for the $D^0 \rightarrow K^- K^+$ decay mode. Events have been selected in the D^0 mass signal region. The dotted line shows the background contribution in the fit. Figure from ⁷⁰.

This expression has three components: R_{DCS} corresponds to the D.C.S. decay rate normalized to the C.F. rate, the term with the quadratic t dependence is due to oscillations whereas the interference between the two processes has a linear time dependence. This expression depends on four parameters: R_{DCS} , $x = \frac{\Delta m}{\Gamma}$, $y = \frac{\Delta \Gamma}{2\Gamma}$ and δ . The last quantity corresponds to a possible strong phase difference for D^0 decaying into $K^- \pi^+$ or $K^+ \pi^-$ respectively. As a result, in Eq. (36), the parameters x' and y' , which are entering, are related to x and y by a rotation of angle δ :

$$x' = x \cos(\delta) + y \sin(\delta) \quad (37)$$

and

$$y' = -x \sin(\delta) + y \cos(\delta) \quad (38)$$

Impressive progress has been made also in the determination of the integrated rate

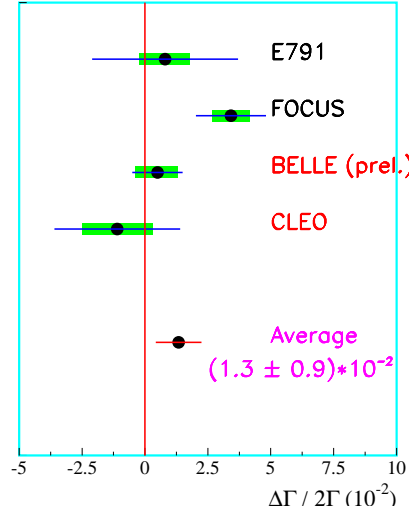


Figure 14. Present measurements of $\frac{\Delta \Gamma}{2\Gamma}$ and global average.

of wrong sign ^c (W.S.) D^0 hadron decays as illustrated in figure 15. New results have been obtained by CLEO ⁷² (figure 16) and BaBar ⁷³ collaborations. Combining the different measurements, R_{WS} is obtained with 10% accuracy. There are also new measurements from CLEO ⁷⁴ on other W.S. D^0 decay channels:

$$R_{WS}(K^- \pi^+ \pi^0) = (0.43_{-0.10}^{+0.11} \pm 0.07) \times 10^{-2} \quad (39)$$

$$R_{WS}(K^- \pi^+ \pi^+ \pi^-) = (0.41_{-0.11}^{+0.12} \pm 0.04) \times 10^{-2} \quad (40)$$

As long as x and y are small, as compared with $\sqrt{R_{DCS}} \simeq \theta_c^2 \simeq 0.05$, the linear term dominates over the last one, in Eq. (36). Integrating over the time variable, results can

^cThe D.C.S. and W.S. rates have to be distinguished. The W.S. rate corresponds to the integral of W.S. events time distribution. For experiments without any bias or limits on the reconstructed D^0 meson proper time: $R_{WS} = R_{DCS} + \sqrt{R_{DCS}} y' + \frac{x'^2 + y'^2}{2}$.

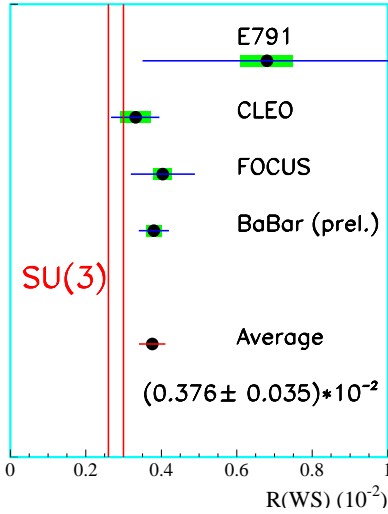


Figure 15. Measurements and global average of wrong sign relative to right sign decay rates of D^0 mesons into $K\pi$. Vertical lines correspond to the naive expectation: $R_{WS} = \tan^4(\theta_c)$.

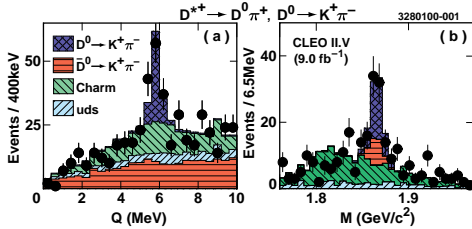


Figure 16. Signal for the W.S. process $D^0 \rightarrow K^+\pi^-$. The data are the full circles with error bars, the projection of the fit for the signal is crosshatched, and the projections of the fit for the backgrounds from charm and light quark production are singly hatched. For part (a), M is within 2σ of the C.F. value, and for (b), $Q = m(K\pi\pi) - m(K\pi) - m(\pi)$ is within 2σ of the C.F. value. Figure from ⁷².

be expressed in the (y', R_{DCS}) plane, see figure 17. In this figure, the CLEO measurement, obtained by fitting R_{DCS} , x' and y' on their registered time distribution has been given along with the constraint obtained by combining wrong-sign rate measurements including all results but CLEO. Within one standard deviation (or so) these results are compatible and also compatible with zero. If the phase δ is not too close to zero (30° or

more) and if x is not much smaller than y , it can be expected that a comparison between the values of y and y' gives access to x . If not, it seems extremely difficult to be sensitive to values of x below 1% because of the quadratic dependence of the last term in Eq. (36). Extracting x from measurements of y and y' requires a determination of δ which seems to be possible at a c -factory ⁷⁵.

In the coming years it can be expected that analyses of W.S. events measured time distributions allow one to reach an accuracy on y' of a few 10^{-3} .

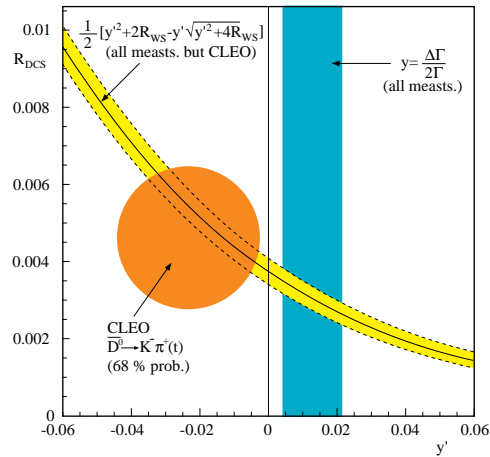


Figure 17. Summary of present measurements in the plane (y', R_{DCS}) . The curved region corresponds to the constraint given by the measured rate of W.S. events, considering that the last term in Eq. (36) has a negligible contribution. The circle is the result from CLEO ⁷² obtained by fitting their measured time distribution (and neglecting the correlation between the two fitted values). The vertical band corresponds to the averaged value of y given in figure 14.

2.5 D^{*+} width measurement

The measurement of the D^{*+} width is challenging because it needs a spectrometer of high resolution and a detailed understanding of its properties. A difficult point comes from the absence of a monitoring channel. In CLEO ⁷⁶, this has been accomplished by performing a detailed comparison between the characteristics of reconstructed and simu-

Sample	Nominal	Kinematic cuts	Tracking quality cuts
# events	11496	3284	368
bad measts.	$\simeq 5\%$	none	none
fitted width (keV)	96.2 ± 4.0	103.8 ± 5.9	104 ± 20
systematics (keV)	± 22	± 20	± 22

Table 6. Summary of the data samples, simulation biases, and fit results.

$$\Gamma(D^{*+}) = \frac{g^2}{24\pi m_{D^*}^2} p_{\pi^+}^3 + \frac{g^2}{48\pi m_{D^*}^2} p_{\pi^0}^3 + \Gamma(D^+\gamma) \quad (41)$$

lated charged particle trajectories. The studied decay chain is: $D^{*+} \rightarrow D^0\pi^+$, $D^0 \rightarrow K^-\pi^+$.

In figure 18, distributions of the variable $Q = m(K^-\pi^+\pi^+) - m(K^-\pi^+) - m(\pi^+)$, for real and simulated events are compared and the value of the intrinsic D^{*+} width is extracted. Typical experimental resolutions on Q are of the order of 150 KeV. Three samples of events, selected with criteria, providing different sensitivities of the measured Q value, to detector properties, due to decay characteristics of the events or to the quality of charged particle reconstruction, have been analysed. They give similar results as indicated in Table 6:

$$\Gamma(D^{*+}) = (96 \pm 4 \pm 22) \text{ KeV} \quad (42)$$

An example of a fitted distribution is given in figure 18.

This measurement is important because it allows one to determine the value of the amplitude for soft pion emission in charm decays:

$$\begin{aligned} g &= g_{D^*D^0\pi^+} = \frac{g_{D^*D^0\pi^+}}{\sqrt{2}} \text{ (isospin)} \\ &= 17.9 \pm 1.9 \end{aligned} \quad (43)$$

The expression relating the D^{*+} total width and g which can be found, for instance in ⁷⁷, is given in Eq. (41).

The amplitude for soft pion emission enters in chiral evaluations and also, as an example, in single pole form factor parametriza-

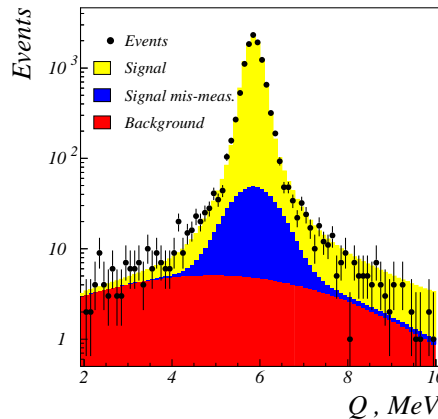


Figure 18. Fit to nominal data sample. The different contributions to the fit are shown. Figure from ⁷⁶.

tions of the semileptonic decay $D \rightarrow \pi\ell^+\nu_\ell$:

$$f_{D\pi}^+(q^2) = \frac{f_{D^*} g}{2m_{D^*}} \left(\frac{1}{1 - \frac{q^2}{m_{D^*}^2}} \right) \quad (44)$$

which can be used when $q^2 \rightarrow m_D^2$ so that the emitted pion is soft. Now the problem comes when the actual result from CLEO is compared with expectations ⁷⁸. Apart for quark models which are in reasonable agreement with the experimental result, but for which it is difficult to attribute an uncertainty, other more QCD-based approaches are failing by a large amount. Light cone sum rules allow one to evaluate the product $f_D f_{D^*} g$ and, separately, f_D and f_{D^*} . They predict ⁷⁹ a rather

low value:

$$\Gamma(D^{*+}) = (35 \pm 20) \text{ KeV} \quad (45)$$

In lattice QCD there is not yet a direct evaluation of g for charm particles. Using their predicted value for the semileptonic form factor at zero recoil ($f_{D\pi}^+(0) = 0.64 \pm 0.05_{-0.07}^{+0.80}$) and Eq. (44) in which the measured value for g is used, a value for the D^{*+} decay constant is obtained: $f_{D^*} = 140 \text{ MeV}$. This value is rather low as compared with expectations of the order of 270 MeV^d . But it must be noted that the result obtained from lattice QCD for $f_{D\pi}^+(0)$ is in rather good agreement with the value deduced from QCD light-cone sum rules and with the experimental measurement of the semileptonic branching fraction $\text{BR}(D^0 \rightarrow \pi^- e^+ \nu_e) = (3.7 \pm 0.6) \times 10^{-3}$ ²³ which, using the parametrization of Eq. (44), corresponds to $f_{D\pi}^+(0) = 0.74 \pm 0.03$. It has to be emphasized that Eq. (44) is expected to be valid at high q^2 whereas the differential decay rate is negligible in this region. Consequently, when comparing the total decay rate with expectations from lattice QCD or QCD sum rules, the q^2 dependence of the form factor is also relevant. Present discrepancies may point to a more complicated q^2 variation than given in Eq. (44). It seems rather important that theorists examine in some detail the present situation.

From the experimental side, it is important also that this measurement be repeated at b -factories, which seem to have similar capabilities as CLEO, and possibly reduce the present systematic uncertainty of $\pm 22 \text{ KeV}$.

2.6 Absolute branching fraction measurements

The present situation²³, summarized in Table 7, needs to be improved a lot.

For exclusive final states, only D^0 decay channels are measured with some accuracy

	Exclusive	$D \rightarrow \ell^+ X$	$D \rightarrow K^- X$
D^0	2.3%	4.5%	8%
D^+	6.7%	11%	12%
D_s	25%	75%	100%
Λ_c^+	26%	?	?
Ξ_c^0	?	?	?
Ξ_c^+	?	?	?
Ω_c^+	?	?	?

Table 7. Present relative accuracies on the best measured c -hadrons exclusive decay channels and on two inclusive processes. The sign “?” indicates that no information is available.

even if the few permil level, reached in τ decays, is far from being accessed. The determination of inclusive properties is really poor. The reason for this situation is very clear. At all $e^+ - e^-$ colliders τ leptons are produced in pairs without any other accompanying particle and thus, absolute branching fraction measurements are a priori possible at all these machines^e. For charm, the only place where c -hadrons are produced in pairs of conjugate states, is in the threshold region. As the present situation is extremely poor and as large statistics of c and b -decays are being registered at CLEO and b -factories, dedicated tagging procedures can be developed and improved results are expected. As an example, the recent measurement, by CLEO⁸¹, of the Λ_c^+ branching fraction into $pK^- \pi^+$ can be given. It is difficult to imagine that such approaches can reach accuracies better than several percent.

The accurate determination of D^+ and D_s decay constants and of the q^2 dependence of form factors in semileptonic decays, which are important measurements to validate lattice QCD calculations can be made only at a Charm factory. This is true also for the determination of inclusive properties

^dIt is expected that $f_{D^*} > f_D \sim 240 \text{ MeV}$.

^eBackground characteristics are not completely negligible as, for instance, the ALEPH²⁰ experiment at LEP has obtained similar precisions as CLEO¹⁹ on the $\tau^- \rightarrow \pi^- \pi^0 \nu_\tau$ channel with ten times less statistics.

of c -hadrons for which, as an example, the most precise results on the D^+ are still coming from MARKIII ⁸².

2.7 D decay constant measurements

A recent result has been obtained by OPAL ⁸³ (see figure 19) and ALEPH ⁸⁴ has also produced a new report. All measurements have been summarized in figure 20. The leptonic branching fraction of charged D mesons is given in Eq. (46) which is similar to the corresponding expression for pions. Because of helicity conservation, the decay rate is proportional to the square of the charged lepton mass. It follows that decays into τ leptons are favoured whereas those into electrons can be neglected. Typical values for expected branching fractions are:

$$\begin{aligned} \text{BR}(D_s \rightarrow \tau^+ \nu_\tau) &= 5.7\%, \\ \text{BR}(D_s \rightarrow \mu^+ \nu_\mu) &= 0.6\%, \\ \text{BR}(D^+ \rightarrow \tau^+ \nu_\tau) &= 0.1\%, \\ \text{BR}(D^+ \rightarrow \mu^+ \nu_\mu) &= 0.04\% \end{aligned} \quad (47)$$

taking $f_{D_d} = 220$ MeV and $f_{D_s} = 260$ MeV. The OPAL analysis ⁸³ is using neural networks to reduce the contamination from $Z \rightarrow b\bar{b}$ events and from other c -hadron decays in $Z \rightarrow c\bar{c}$ events. Evidence for the signal is obtained using the cascade decay $D_s^* \rightarrow D_s \gamma$ (see figure 19).

The average value for f_{D_s} , taking into account correlated systematic uncertainties which are dominated by the error on the $D_s \rightarrow \phi \pi^+$ branching fraction, is equal ^f to:

$$f_{D_s} = (267 \pm 7^{+31}_{-35}) \text{ MeV} \quad (48)$$

and agrees with lattice QCD evaluations which correspond to $f_{D_s}(\text{lattice}) = (250 \pm 25)$ MeV ⁸⁶. Such a comparison is expected to be a stringent test for lattice QCD as measurements of D meson decay constants can

^fA rather similar value: $f_{D_s} = (264 \pm 15 \pm 33)$ MeV can be found in ⁸⁵.

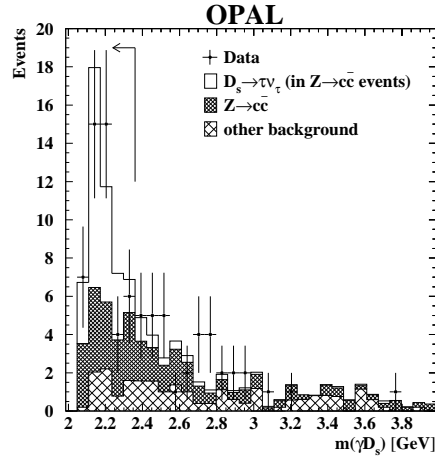


Figure 19. Invariant mass $m(\gamma D_s)$ of the photon and the D_s candidate for the events satisfying all selection criteria. The contributions to the Monte Carlo distribution from the signal and from the different sources of background are shown separately. The signal region is indicated by an arrow. Figure from ⁸³.

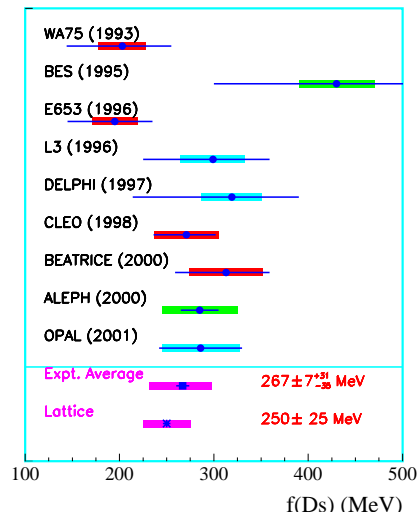


Figure 20. Summary of experimental results on the D_s decay constant. Measurements of $D_s \rightarrow \tau^+ \nu_\tau$ and $D_s \rightarrow \mu^+ \nu_\mu$ decay rates have been combined.

$$\text{BR}(D_{s,d} \rightarrow \ell^+ \nu_\ell) = \frac{G_F^2}{8\pi} \tau(D_{s,d}) f_{D_{s,d}}^2 |V_{c(s,d)}|^2 m_{D_{s,d}} m_\ell^2 \left(1 - \frac{m_\ell^2}{m_{D_{s,d}}^2}\right)^2 \quad (46)$$

reach a percent accuracy at a Charm facility. Obtaining values of B meson decay constants from extrapolations of measured D decay constants could be a valuable approach⁵¹ as it is impossible, in practice, to measure directly f_B .

3 Conclusions

As you have noted τ and charm physics are on very different grounds. They are extremely nice laboratories to study QCD in its perturbative and non-perturbative aspects. These properties have been already well exploited in τ decays whereas, for charm, a lot remains to be done.

The two aspects are complementary. In τ decays the production of hadrons is clean and simple, through the charged weak current. This allows one to control non-perturbative contributions and to access fundamental parameters of the theory such as α_s and quark masses. In charm decays, the hadronic current is coupled to a heavy quark (charm). Simple situations met in leptonic and semileptonic decays allow one to control lattice QCD evaluations of heavy meson decay constants and form factors. Accurate measurements in these domains need the use of a charm factory. This will open a basic understanding of non-perturbative QCD for the benefit of, for instance, the extraction of CKM matrix element values from measurements of b -hadron decays or oscillations.

Acknowledgments

I would like to thank all members of the different Collaborations who sent me new results, in time for the Conference. I apologize for not having been able to give a complete account of all their achievements. I thank A.

Le Yaouanc for having explained to me the different problems raised by the CLEO measurement of the D^* width and R. Rückl for his comments on this subject. I have benefited also of useful comments from I.I. Bigi, especially on charm lifetime measurements and from M. Davier and A. Pich on the τ aspect of this presentation. I thank the organizers of the Conference for their invitation and support. Special thanks to Mario Antonelli for his help during the Conference. Merci également à C. Bourge pour son aide technique durant l'élaboration de ce document.

References

1. P. Abreu *et al.*, DELPHI Collaboration, Eur. Phys. J. **C16** (2000) 229.
2. F. Matorras and D. Reid, DELPHI Collaboration, DELPHI 2001-091 CONF 519.
3. A. Heister *et al.*, ALEPH Collaboration, Eur. Phys. J. **C20** (2001) 401.
4. P. Abreu *et al.*, DELPHI Collaboration, Eur. Phys. J. **C14** (2000) 585.
5. M. Acciari *et al.*, L3 Collaboration, Phys. Lett. **B429** (1998) 387.
6. G. Alexander *et al.*, OPAL Collaboration, Z. Phys. **C72** (1996) 365.
7. K. Abe *et al.*, SLD Collaboration, Phys. Rev. Lett. **84** (2000) 5945.
8. See:
<http://lepewwg.web.cern.ch/LEPEWWG/>
9. T. van Ritbergen and R.G. Stuart, Phys. Rev. Lett. **82** (1999) 488.
10. S.H. Robertson, Invited talk presented at the 6th International Workshop on Tau Lepton Physics (TAU 00), Nucl. Phys. Proc. Suppl. **98** (2001) 67.
11. R. Decker and M. Finkemeier, Nucl. Phys. **B438** (1995) 17.
12. A. Andreazza, C. Meroni and R. Mc

- Nulty, DELPHI 2001-090 CONF 518.
13. J.Z. Bai *et al.*, BES Collaboration, Phys. Rev. **D53** (1996) 20.
 14. A. Pich and J. Portolés, Phys. Rev. **D63** (2001) 093005.
 15. J. Bijnens, Chiral Lagrangians, hep-ph/0108111.
 16. L. M. Barkov *et al.*, Nucl. Phys. **B256** (1985) 365.
 17. S. R. Amendolia *et al.*, Nucl. Phys. **B277** (1986) 168.
 18. F. Guerrero and A. Pich, Phys. Lett. **B412** (1997) 382.
 19. S. Anderson *et al.*, CLEO Collaboration, Phys. Rev. **D61** (2000) 112002.
 20. R. Barate *et al.*, ALEPH Collaboration, Z. Phys. **C76** (1997) 15.
 21. R.R. Akhmetshin *et al.*, Preprint Budker INP99-10, Novosibirsk, 1999.
 22. S.I. Eidelman, Invited talk presented at the 6th International Workshop on Tau Lepton Physics (TAU 00), Nucl. Phys. Proc. Suppl. **98** (2001).
 23. D.E. Groom *et al.* Eur. Phys. J. **C15** (2000) 1.
 24. D. Buskulic *et al.*, ALEPH Collaboration, Phys. Lett. **B307** (1993) 209.
 25. E. Braaten, S. Narison and A. Pich, Nucl. Phys. **B373** (1992) 581; F. Le Diberder and A. Pich, Phys. Lett. **B286** (1992) 147; *ibid* Phys. Lett. **B289** (1992) 165.
 26. M. A. Shifman, A. L. Vainshtein and V. I. Zakharov, Nucl. Phys. **B147** (1979) 385, 448, 519.
 27. W.J. Marciano and A. Sirlin, Phys. Rev. Lett. **61** (1988) 1815.
 28. E. Braaten and C.S. Li, Phys. Rev. **D42** (1990) 3888.
 29. T. Coan *et al.*, CLEO Collaboration, Phys. Lett. **B356** (1995) 580.
 30. R. Barate *et al.*, ALEPH Collaboration, Eur. Phys. J. **C4** (1998) 409.
 31. A. Rougé, Z. Phys. **C70** (1996) 65.
 32. K. Ackerstaff *et al.*, OPAL Collaboration, Eur. Phys. J. **C7** (1999) 571.
 33. R. Barate *et al.*, ALEPH Collaboration, Eur. Phys. J. **C4** (1998) 409.
 34. R. Barate *et al.*, ALEPH Collaboration, Eur. Phys. J. **C1** (1998) 65; Eur. Phys. J. **C4** (1998) 29; Eur. Phys. J. **C10** (1999) 1.
 35. S. J. Richichi *et al.*, CLEO Collaboration, Phys. Rev. **D60** (1999) 112002; D.M. Asner *et al.*, CLEO Collaboration, Phys. Rev. **D62** (2000) 072006.
 36. G. Abbiendi *et al.*, OPAL Collaboration, Eur. Phys. J. **C13** (2000) 197; Eur. Phys. J. **C13** (2000) 213; Eur. Phys. J. **C19** (2001) 653.
 37. R. Barate *et al.*, ALEPH Collaboration, Eur. Phys. J. **C11** (1999) 599.
 38. K. Maltman and J. Kambor, Phys. Rev. **D62** (2000) 093023; *ibid*, Phys. Rev. **D64** (2001) 093014.
 39. S. Chen, M. Davier, E. Gámiz, A. Höcker, A. Pich and F. Prades, hep-ph/0105253.
 40. J. G. Körner, F. Krajewski and A. A. Pivovarov, Eur. Phys. J. **C20** (2001) 259.
 41. G. Amoros, J. Bijnens and P. Talavera, Nucl. Phys. **B602** (2001) 87.
 42. H. N. Brown *et al.*, Muon g-2 Collaboration, Phys. Rev. Lett. **86** (2001) 2227.
 43. S. Eidelman and F. Jegerlehner, Z. Phys. **C67** (1995) 585.
 44. M. Davier and A. Höcker, Phys. Lett. **B419** (1998) 419.
 45. S. Adler, Phys. Rev. **D10** (1974) 3714.
 46. S. Groote, J.G. Körner, K. Schilcher and N.F. Nasrallah, Phys. Lett. **B440** (1998) 375.
 47. M. Davier and A. Höcker, Phys. Lett. **B435** (1998) 427.
 48. J.F. de Trocóniz and F.J. Ynduráin, hep-ph/0106025.
 49. J. Z. Bai *et al.* BES Collaboration, hep-ex/0102003.
 50. I.I. Bigi, Summary talk given at 5th Workshop on Heavy Quarks at Fixed Target (HQ2K), Rio de Janeiro, Brazil,

- 9-12 Oct 2000; hep-ph/0012161.
51. P. Paganini, F. Parodi, P. Roudeau and A. Stocchi, Phys. Scripta **58** (1998) 556.
 52. E. M. Aitala *et al.*, E791 Collaboration, Phys. Rev. Lett. **86** (2001) 765; C. Göbel, E791 Collaboration, hep-ex/0012009.
 53. G. Bellini, I. I. Bigi and P. J. Dornan, Phys. Rep. **289** (1997) 1.
 54. K. Abe *et al.*, BELLE Collaboration, BELLE-CONF-0131.
 55. A. H. Mahmood *et al.*, CLEO Collaboration, Phys. Rev. Lett. **86** (2001) 2232.
 56. J. M. Link *et al.*, FOCUS Collaboration, Phys. Lett. **B485** (2000) 62.
 57. M. Iori *et al.*, SELEX Collaboration, hep-ex/0106005.
 58. I.I. Bigi and N.G. Uraltsev, Z. Phys. **C62** (1994) 623.
 59. M.B. Voloshin, Phys. Lett. **B385** (1996) 369.
 60. M. Artuso *et al.*, CLEO Collaboration, CLEO CONF 01-03; hep-ex/0107040.
 61. J.M. Link *et al.*, FOCUS Collaboration, hep-ex/0110002.
 62. I.I. Bigi and A.I. Sanda, Phys. Lett. **B171** (1986) 320.
 63. F. Buccella *et al.*, Phys. Rev. **D51** (1995) 3478.
 64. A.J. Schwartz, E791 Collaboration, International Conference on CP Violation Physics, Ferrara, Italy, 18-22 Sep 2000; Nucl. Phys. Proc. Suppl. **99A** (2001) 276; hep-ex/0012006.
 65. A.B. Smith, CLEO Collaboration, 4th International Conference on B Physics and CP Violation (BCP 4), Ago Town, Mie Prefecture, Japan, 19-23 Feb 2001; hep-ex/0104008.
 66. S. Bianco, FOCUS Collaboration, International Conference on CP Violation Physics, Ferrara, Italy, 18-22 Sep 2000; Nucl. Phys. Proc. Suppl. **99A** (2001) 191; hep-ex/0011055.
 67. G. Burdman, hep-ph/9407378 and references therein.
 68. I.I. Bigi and N.G. Uraltsev, Nucl. Phys. **B592** (2001) 92.
 69. A.A. Petrov, 4th Workshop on Continuous Advances in QCD, Minneapolis, Minnesota, 12-14 May 2000, hep-ph/0009160; A. F. Falk, Y. Grossman, Z. Ligeti and A. A. Petrov, hep-ph/0110317.
 70. K. Abe *et al.*, BELLE Collaboration, BELLE-CONF-0131.
 71. J.M. Link *et al.*, FOCUS Collaboration, Phys. Lett. **B485** (2000) 62.
 72. R. Godang *et al.*, CLEO Collaboration, Phys. Rev. Lett. **84** (2000) 5038.
 73. BaBar Collaboration, result submitted at this Conference.
 74. G. Brandenburg *et al.*, CLEO Collaboration, CLNS 01/1731; S.A. Dytman *et al.*, CLEO Collaboration, CLNS 01/1748.
 75. M. Gronau, Y. Grossman and J.L. Rosner, Phys. Lett. **B508** (2001) 37.
 76. T.E. Coan *et al.*, CLEO Collaboration, CLEO CONF 01-2.
 77. M.B. Wise, Phys. Rev. **D45** (1992) R2188.
 78. D. Becirevic, A. Le Yaouanc, J. of High Ener. Phys. **03** (1999) 21; hep-ph/9901431.
 79. V.M. Belyaev, V.M. Braun, A. Khodjamirian and R. Rückl, Phys. Rev. **D51** (1995) 6177.
 80. A. Abada, D. Becirevic, P. Boucaud, J.P. Leroy, V. Lubicz, G. Martinelli, F. Mescia; 7th International Symposium on Lattice Field Theory (LATTICE 99), Pisa, Italy, 29 Jun - 3 Jul 1999; Nucl. Phys. Proc. Suppl. **83** (2000) 268; hep-lat/9910021.
 81. D.E. Jaffe *et al.*, CLEO Collaboration, Phys. Rev. **D62** (2000) 072005.
 82. R.M. Baltrusaitis *et al.*, MARKIII Collaboration, Phys. Rev. Lett. **54** (1985) 1976.
 83. G. Abbiendi *et al.*, OPAL Collaboration, Phys. Lett. **B516** (2001) 236.
 84. ALEPH Collaboration, ALEPH 2001-

051, CONF 2001-031.

85. S. Söldner-Rembold, HEP 2001 Conference (Budapest), hep-ex/0109023.
86. M. Ciuchini, G. D'Agostini, E. Franco, V. Lubicz, G. Martinelli, F. Parodi, P. Roudeau and A. Stocchi, RM3-TH/01-10.